DOI: 10.1002/ejic.201100365

Crystalline and Liquid Crystalline Organic–Inorganic Hybrid Salts with Cation-Sensitized Hexanuclear Molybdenum Cluster Complex Anion Luminescence

Joanna Bäcker,[a] Svenja Mihm,[b] Bert Mallick,[a] Mei Yang,[a] Gerd Meyer,*[b] and Anja-Verena Mudring*[a]

Dedicated to Professor John D. Corbett on the occasion of his 85th birthday

Keywords: Cluster compounds / Ionic liquids / Liquid crystals / Luminescence / Synthesis design

The salts $[C_n\text{mim}]_2[Mo_6Cl_{14}]$ (mim = methylimidazolium; n = 4, 6, 12, 16, 18) have been obtained by reaction of $C_n$mimCl with $MoCl_2$. Thermal analysis shows the melting point decreases with increasing alkyl chain length of the cation. The imidazolium chloromolybdates(II) with n = 6–18 decompose above 340 °C; $[C_{18}\text{mim}]_2[Mo_6Cl_{14}]$ is thermally stable up to 390 °C. All compounds are insensititve to the constituents of the atmosphere. Of the higher melting salts $[C_n\text{mim}]_2[Mo_6Cl_{14}]$ (n = 4, 6), high-quality single crystals could be obtained. Single-crystal X-ray structural analyses clearly show that the cluster complex anion $[Mo_6Cl_{14}]^{2-}$ has an electron-precise octahedral $\{Mo_6\}$ cluster. For $[C_4\text{mim}]_2[Mo_6Cl_{14}]$, two polymorphs differing in the cation alkyl-side-chain conformation were obtained. The less thermodynamically stable modification with a *gauche* conformation undergoes monotropic phase transition to the more stable form with the all-*trans* conformation. Long alkyl-side-chain salts, $[C_n\text{mim}]_2[Mo_6Cl_{14}]$ with n = 16 and 18, exhibit thermotropic liquid-crystalline behaviour. All compounds show bright red luminescence centred at about 730 nm with a lifetime of about 0.15 ms, originating from the cluster complex anion, which can be sensitized by the imidazolium cations.

Introduction

Halides of heavier Group 5 and 6 metals in lower oxidation states show an extensive tendency towards metal–metal bonding.[1] It was a big surprise when structure determination of the light yellow salt of $MoCl_2$ exhibited octahedra of molybdenum atoms, $\{Mo_6\}$, surrounded by eight face-capping [μ_3, or i for "innere Liganden" (inner ligands)] and six terminal [over the vertices, μ_1, or a for "äußere Liganden" (outer ligands)] chloride ligands.[2] The $[\{Mo_6\}Cl^i_8Cl^a_6]^{2-}$ cluster complexes need to share four a-type ligands to achieve the composition $MoCl_2 = \{Mo_6\}Cl_{12} = \{Mo_6\}Cl^i_{8/1}Cl^a_{2/1}Cl^{a-a}_{4/2}$.[1a,3] The $\{Mo_6\}$ cluster is understood to be an electron-precise 24-electron cluster in the sense that 24 electrons are available for intra-cluster bonding;[4] in a molecular orbital (MO) view these occupy 12 bonding orbitals, leaving a rather wide gap to the anti-bonding LUMO (see below for luminescence). The occupation of 12 bonding, cluster-based orbitals clearly accounts for a very stable cluster and, thus, a very stable anionic cluster complex, $[\{Mo_6\}Cl_{14}]^{2-}$, because $\{Mo_6\}Cl_{12}$ may be dissolved in hydrochloric acid and salts may be crystallized from such a solution. $Hg[\{Mo_6\}Cl_{14}]$ was perhaps the first cluster complex salt to be structurally characterized by single-crystal X-ray diffraction.[5] Many characterizations have followed, either homo- or heteroleptic salts of the $[\{Mo_6\}L^i_8L^a_6]^{2-}$ cluster complex anion[6] (Figure 1).

The anion $[\{Mo_6\}Cl_{14}]^{2-}$ is a large anion with a diameter of about 1 nm. Crystallization from solution can be accomplished with a large variety of cations, not only simple mono- or divalent cations, such as Cs^+ or Hg^{2+}, but – even more advantageous for better crystallization – large cations, such as $[Ca(dmso)_6]^{2+}$ or $[Rb(12c4)_2]^+$ (12c4 = 12-crown-4).[6c] A large variety of solvents and solvent mixtures have been tested for crystallization, not only aqueous solutions, but also polar organic solvents, such as alcohols, dimethyl sulfoxide or acetonitrile, may be used.

Molten salts, especially imidazolium-based tetrachloroaluminates have also been used as solvents, even at room temperature.[7] At present, this molten salt chemistry is ex-

[a] Fakultät für Chemie, Anorganische Chemie I – Festkörperchemie und Materialien, Ruhr-Universität Bochum, 44780 Bochum, Germany
Fax: +49-234-32-14951
E-mail: anja.mudring@rub.de
[b] Department für Chemie, Lehrstuhl für Anorganische Festkörper- und Koordinationschemie, Universität zu Köln, Greinstraße 6, 50939 Köln, Germany
Fax: +49-221-470-5083
E-mail: gerd.meyer@uni-koeln.de
Supporting information for this article is available on the WWW under http://dx.doi.org/10.1002/ejic.201100365.

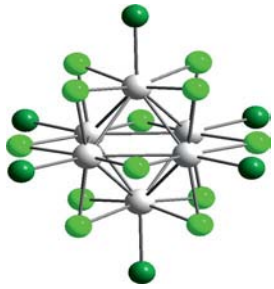

Figure 1. Ball-and-stick model of the anionic cluster complex $[\{Mo_6\}L^i_8L^a_6]^{2-}$; ligands L^i (light green) and L^a (dark green) may or may not be identical.

periencing a revival through applications in ionic-liquid (IL) chemistry,[8] with a large variety of cations and anions. With the incorporation of complex f-metal anions in ionic liquids, a new generation of ILs with interesting properties, such as luminescence or magnetism, have become accessible.[9] Likewise, d-element ions in ILs give rise to auspicious properties.[10] Typically, the complex metal anion is obtained by dissolving the respective binary metal salt in an IL containing the same anion. In this context, salts such as $MoCl_2$, which contain a stable metal cluster complex (see above), drew our attention. We have, therefore, undertaken a more systematic study of the dissolution of $MoCl_2$ in alkylimidazolium chloride ILs $[C_n\text{mim}]Cl$ (mim = methylimidazolium; n = 4, 6, 12, 16, 18) with the aim of evaluating whether it is possible to obtain ILs or low melting salts with the cluster complex anion $[\{Mo_6\}Cl_{14}]^{2-}$.

Results and Discussion

Syntheses

The reactions of five alkylimidazolium chlorides $[C_n\text{mim}]Cl$ (n = 4, 6, 12, 16, 18) with $MoCl_2$ were carried out in Schlenk tubes under vacuum at 100–110 °C for 3 d. Yellow to orange salts of $[C_n\text{mim}]_2[Mo_6Cl_{14}]$ solidified upon cooling to ambient temperature. Compounds with alkyl chains with n = 12, 16, 18 (compounds **3**, **4**, and **5**, respectively) were wax-like and their wax-like behaviour increased with increasing alkyl chain length. High-quality single crystals of compounds with shorter alkyl chains, $[C_4\text{mim}]_2[Mo_6Cl_{14}]$ (**1a** and **1b**) and $[C_6\text{mim}]_2[Mo_6Cl_{14}]$ (**2**), were obtained and allowed X-ray structure analyses. Compounds **1a** and **1b** were synthesized and crystallized independently in pure phases by using slightly different synthetic procedures.

Single-Crystal X-ray Structures

Selected crystallographic data for **1a**, **1b** and **2** are summarized in Table 1. Comparison of measured X-ray powder patterns and those calculated with crystal structure data of **1a**, **1b** and **2** confirm the correctness of the structure solutions and the phase purity of the compounds. Compounds **1a**, **1b** and **2** all feature the complex cluster anion $[\{Mo_6\}Cl^i_8Cl^a_6]^{2-}$. Mo–Mo, Mo–$Cl^i$, and Mo–$Cl^a$ distances correspond very well with those statistically found for a large number of salts with the $[\{Mo_6\}Cl_{14}]^{2-}$ anion.[6c]

Table 1. Crystallographic data for $[C_n\text{mimCl}]_2[Mo_6Cl_{14}]$ with n = 4 (**1a**, **1b**) and n = 6 (**2**); the space group is $P2_1/c$ (no. 14) in all cases.

	1a	**1b**	**2**
a [pm]	991.1(5)	982.6(1)	1176.8(2)
b [pm]	1684.3(8)	1826.6(2)	1012.1(2)
c [pm]	1186.4(5)	1147.8(1)	1908.9(4)
β [°]	111.010(9)	109.59(13)	107.64(1)
V [Å^3]	1849(2)	1940.4(4)	2166.0(8)
T [K]	153(2)	293(2)	293(2)
$R1$ [%]	5.58	3.18	2.75
$wR2$ [%]	14.5	4.70	5.95
Goof	1.14	0.722	0.952

Distances and angles in the n-alkyl-methylimidazolium cation of **1a**, **1b** and **2** (Table 2) are the same as those commonly observed.[11] However, there are distinct differences in the conformation of the cations. For compounds **1a** and **1b**, the main difference is the conformation of the butyl side chain of the imidazolium cation (Figure 2). In **1a** a *gauche* conformation is found along the C5–C6 bond, whereas **1b** features only *anti* conformations. Furthermore, the orientation of the alkyl chain with respect to the imidazolium ring plane is different. In **1a** the alkyl chain is oriented backwards with an (N2–C5–C6) angle of –111.85(2)°, in **1b** it is forward with an angle of 113(1)°. The hexyl side chain in **2** also features only *anti*-conformations and bends backwards with an angle of –111.67(1)°.

Table 2. Selected interatomic distances for **1a**, **1b** and **2**.

1a	d [Å]	**1b**	d [Å]	**2**	d [Å]
Mo1–Cl1^a	2.432(6)	Mo1–Cl1^a	2.418(4)	Mo1–Cl1^a	2.43(1)
Mo1–Cl4^i	2.471(6)	Mo1–Cl4^i	2.47(2)	Mo1–Cl6^i	2.47(1)
Mo1–Cl7^i	2.473(8)	Mo1–Cl5^i	2.471(2)	Mo1–Cl7^i	2.47(3)
Mo1–Cl6^i	2.473(7)	Mo1–Cl7^i	2.474(2)	Mo1–Cl4^i	2.47(1)
Mo1–Cl5^i	2.476(8)	Mo1–Cl6^i	2.48(2)	Mo1–Cl5^i	2.48(2)
Mo2–Cl2^a	2.427(2)	Mo2–Cl2^a	2.42(2)	Mo2–Cl2^a	2.43(4)
Mo2–Cl7^i	2.47(1)	Mo2–Cl5^i	2.46(1)	Mo2–Cl4^i	2.43(4)
Mo2–Cl4^i	2.49(1)	Mo2–Cl4^i	2.467(2)	Mo2–Cl7^i	2.47(1)
Mo2–Cl5^i	2.479(2)	Mo2–Cl7^i	2.468(2)	Mo2–Cl5^i	2.47(2)
Mo2–Cl6^i	2.483(2)	Mo2–Cl6^i	2.48(1)	Mo2–Cl6^i	2.47(2)
Mo3–Cl3^a	2.42(2)	Mo3–Cl3^a	2.436(6)	Mo3–Cl3^a	2.42(3)
Mo3–Cl4^i	2.467(3)	Mo3–Cl7^i	2.463(9)	Mo3–Cl7^i	2.47(1)
Mo3–Cl5^i	2.472(2)	Mo3–Cl5^i	2.47(1)	Mo3–Cl5^i	2.47(4)
Mo3–Cl7^i	2.474(6)	Mo3–Cl6^i	2.474(9)	Mo3–Cl4^i	2.48(1)
Mo3–Cl6^i	2.477(5)	Mo3–Cl4^i	2.478(8)	Mo3–Cl6^i	2.48(4)
Mo1–Mo2	2.607(5)	Mo1–Mo3	2.599(1)	Mo1–Mo2	2.60(2)
Mo1–Mo3	2.610(2)	Mo1–Mo2	2.602(9)	Mo1–Mo2	2.60(4)
Mo1–Mo3	2.610(2)	Mo1–Mo2	2.604(9)	Mo1–Mo2	2.60(1)
Mo1–Mo2	2.613(2)	Mo1–Mo3	2.61(1)	Mo1–Mo3	2.609(9)

Views of the crystal structures of **1a**, **1b** and **2** along the two shorter crystallographic axes (Figure 3) show that the packing of imidazolium cations and $[\{Mo_6\}Cl_{14}]^{2-}$ anions, in a 2:1 ratio, is very similar for these compounds. However, the relative orientation of the $[C_4\text{mim}]^+$ cations and the $[\{Mo_6\}Cl_{14}]^{2-}$ anions are slightly different for **1a** and **1b**. The layers are farther apart in **1b** than those in **1a** which is attested by the longer b axis, 1684.3(8) versus 1826.6(2) pm

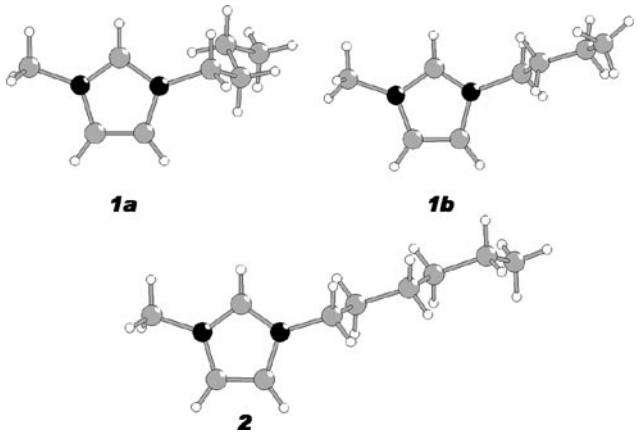

Figure 2. Conformations of the *n*-alkyl-methylimidazolium cations in the crystal structures of **1a**, **1b** and **2**.

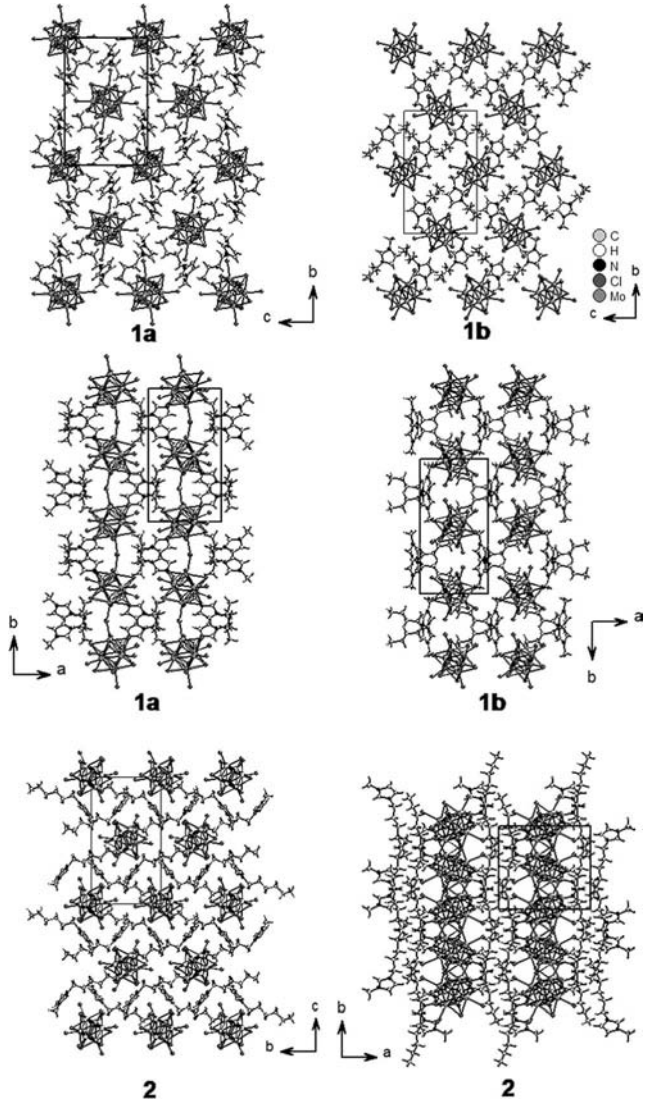

Figure 3. Projections of the crystal structures of $[C_n\text{mim}]_2[Mo_6Cl_{14}]$ with $n = 4$ (**1a**, **1b**) and $n = 6$ (**2**) showing the packing of cations and anions in two different directions.

(**1a** vs. **1b**). Quite clearly, the all-*anti* butyl chains in **1b** are more voluminous. Indeed, the cell volume of **1b** is larger than that of **1a**, hence the density of **1a** (2.426 $g\,cm^{-3}$) is larger than that of **1b** (2.311 $g\,cm^{-3}$). The effect on the structure of extending the alkyl chain by two carbon atoms becomes evident when comparing the structures of **1a**/**1b** and **2** (Figure 3). In all three cases, cationic and anionic layers alternate along [100] and they become more separated with the length of the alkyl chains.

IR Spectroscopy

IR spectra for all $[C_n\text{mim}]_2[Mo_6Cl_{14}]$ compounds investigated in this work show the characteristic vibrations of the cations (see the Supporting Information). Between 2870 and 3165 cm^{-1}, the stretching modes for sp^3- and sp^2-C–H vibrations are observed. The C=N and C=C stretching modes are found at around 1572 cm^{-1}. Furthermore, a C–H deformation mode can be observed at about 1466 cm^{-1}. A comparison of the IR spectra of **1a** and **1b** shows additional modes for **1b** in the region where C–C modes are active at 1258 and 1030 cm^{-1}. This may be attributed to the mixed *anti-gauche* conformation of the alkyl chain of the methylimidazolium cation in **1b**, compared with the all-*trans* conformation in **1a**. These vibrations are absent in the IR spectrum of $[C_6\text{mim}]_2[Mo_6Cl_{14}]$ (**3**), and indeed, the solid-state structure shows the cation to be in the all-*trans* conformation. However, they start to appear again in the compounds with longer alkyl chains; an indication of mixed conformations of the longer alkyl chains.

Thermal Behaviour

All $[C_n\text{mim}]_2[Mo_6Cl_{14}]$ compounds investigated herein show surprisingly high decomposition points (Tables 3 and 4; for a graphical display of the TG curves see the Supporting Information). It seems that the low Lewis basicity of the $[Mo_6Cl_{14}]^{2-}$ cluster anion is responsible for the high thermal stability.

Table 3. Thermal data for $[C_n\text{mim}]_2[Mo_6Cl_{14}]$ ($n = 4$, 6, 12).

		1a, **b**		**2**		**3**	
		T [°C]	Δ*H* [kJ mol^{-1}]	*T* [°C]	Δ*H* [kJ mol^{-1}]	*T* [°C]	Δ*H* [kJ mol^{-1}]
Heating	ss[a]	126.3 (**1a**)	6.0				
	m	226.7	43.05	226.2	50.17	167.2	15.02
Cooling	c	200.5	–37.58	139.4	–23.1	123.5	–15.04
Heating	d	354		354		344	

[a] s = monotropic solid–solid phase transition, m = melting, c = crystallization, d = decomposition.

With respect to their thermal behaviour, below the decomposition point the compounds can be grouped in two classes. Compounds **1**–**3** show distinct melting and crystallization [graphical representations of the differential scanning calorimetry (DSC) traces can be found in the Supporting Information]. Compounds **1** and **2** both melt at around

Table 4. Thermal data for $[C_n mim]_2[Mo_6Cl_{14}]$ (n = 16, 18).

		4		**5**	
		T [°C]	ΔH [kJ mol^{-1}]	T [°C]	ΔH [kJ mol^{-1}]
Heating (2nd)	G–M[a]	–0.1	7.0	–31.0	
		83.4	–25.51	62.9	–41.53
	M–M	132.6	25.61	133.0	28.35
	M–L	159.8	14.80	147.8	6.57
Cooling (1st)	L–M	144.2	–17.41	123.1	–8.12
	M–M	140.7	–0.73	101.7	–9.37
	M–G	–5.6	–5.82	–37.9	
Heating	d	351		390	

[a] G–M = glass–mesophase transition, M–M = mesophase–mesophase transition, M–L = mesophase–liquid transition, d = decomposition.

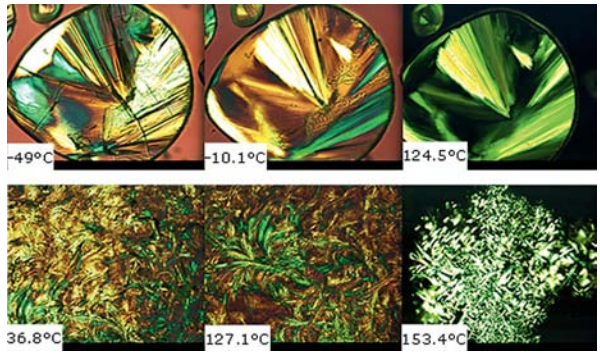

Figure 4. Defect textures of the LC states of **4** (top) and **5** (bottom) as observed by POM when cooling the isotropic melt at the respective temperatures.

226–227 °C. However, compound **1** crystallizes more readily, whereas **2** shows a substantial supercooling of –90 °C before it crystallizes. Compound **3** shows a significantly lower melting point than **1** and **2** and the degree of supercooling (≈ 45 °C) is less than that of **2**. Thus, it appears that longer alkyl chains kinetically hamper crystallization. Compound **1a** shows a monotropic phase transition into **1b** at 126.3 °C. After this temperature, the thermal behaviour of the sample is identical to that of **1b**. Modification **1b** is, therefore, the thermodynamically more stable modification, although with a rather small enthalpy of transformation of only 6 kJ mol^{-1}. This behaviour can be attributed to the conformation of the butyl chain, which is *all-anti* in **1b**.

The phase behaviour of the long-alkyl-chain compounds **4** and **5** is far more complex. Compounds **4** and **5** melt to form isotropic liquids at 159.8 and 147.8 °C, respectively. Thus, the tendency, already observed for **1**–**3**, for the melting point to decrease with the length of the alkyl chain on the imidazolium cation is followed further. However, upon cooling from the isotropic melt, neither **4** nor **5** crystallizes. Rather, both form liquid-crystalline (LC) phases. Figure 4 displays the defect textures observed by polarizing optical microscopy (POM) for the two compounds at the respective temperatures. Subtle changes of the defect texture can be seen, which are mirrored by the small enthalpy changes in the DSC. For both compounds, a mesophase–mesophase transition is observed above 100 °C.

Small-angle X-ray scattering (SAXS) experiments show, for the high-temperature mesophase, repeating units of about 27.4 and 26.6 Å for $[C_{16}mim]_2[Mo_6Cl_{14}]$ and 36.5 and 33.3 Å for $[C_{18}mim]_2[Mo_6Cl_{14}]$, which shift with temperature, according to thermal expansion and contraction (for diffraction patterns taken at various temperatures, see the Supporting Information). Below the mesophase–mesophase phase transition, only one repeating distance can be detected in the SAXS area: at about 29.4 Å for $[C_{16}mim]_2[Mo_6Cl_{14}]$ and 32.2 Å for $[C_{18}mim]_2[Mo_6Cl_{14}]$. The latter distances roughly amount to the diameter of one complex anion plus the length of the respective cation. The POM and SAXS observations are in agreement with the formation of a highly ordered hexagonal LC phase, which converts to a rectangular one at higher temperatures.

It seems that none of the compounds form a complete crystalline state upon cooling. The cracks in the material, which the POM image shows for **4** at –49 °C, evidently result from mechanical stress. However, the LC texture is still present, which illustrates that the material freezes into a semi-ordered state. Upon heating, when enough thermal energy becomes available, partial ordering sets in at some point, as observed by the exothermic events present in both heating curves of **4** and **5**.

Optical Spectroscopy

The optical properties of compounds **1**–**5** were studied by UV/Vis absorption and luminescence spectroscopy. The distinct absorption maxima determined by UV/Vis absorption spectroscopy (see the Supporting Information) agree very well with the observed yellow–orange colour of the compounds, as commonly found for compounds with the $[\{Mo_6\}Cl_{14}]^{2-}$ cluster complex anion.[12] The absorption maxima appear at the same value as the first maximum observed in the excitation spectrum and seem to be independent of the countercation. The corresponding electronic transitions can be attributed to intra-cluster transitions. However, a second transition is found in the excitation spectrum at lower energies, which depends on the cation. In this area, inter-cluster transitions also take place—as observed for $MoCl_2$ itself—as well as the allowed $^1\pi$–$^1\pi^*$ and forbidden $^1\pi$–$^3\pi^*$ transitions within the imidazolium cation[13] (see the Supporting Information). All transitions have a rather short lifetime and cannot be well separated by time-resolved measurements. With increasing alkyl chain length at the cation a blueshift from 489 nm for **1** to 458 nm for **5** is observed (for further details see the Supporting Information).

In the emission spectrum no cation emission can be observed, indicating efficient energy transfer between the imidazolium cation and the $[\{Mo_6\}Cl_{14}]^{2-}$ cluster complex anion. Upon excitation at both 360 (excitation into the complex cluster anion levels) and 475 nm (excitation into the imidazolium head group), all compounds show a bright red emission centred at around 730 nm (Figure 5). This emission is typical for electronic transitions within the $[\{Mo_6\}Cl_{14}]^{2-}$ cluster anion. It agrees well with observa-

tions for other compounds containing the $[\{Mo_6\}Cl_{14}]^{2-}$ cluster anion, such as the starting material $MoCl_2$,[14] and with theoretical calculations.

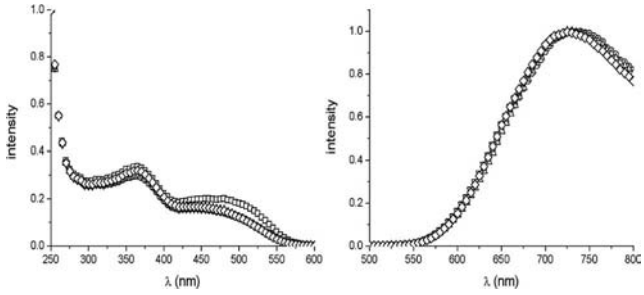

Figure 5. Comparison of the excitation spectra, monitored at 730 nm (left) and emission spectra, obtained upon excitation at 360 nm (right) of **1** (□), **2** (○), **3** (Δ), **4** (∇), and **5** (◇).

Lifetimes of the excited states for **1**–**5** of 0.154 to 0.132 ms at room temperature correspond to typical values for the cluster anion.[15] To a first approximation, the lifetime of the excited state becomes shorter with increasing alkyl chain length due to increased vibronic quenching.

Conclusions

Alkyl-methylimidazolium chlorides, $[C_n\text{mim}]Cl$ with n = 4, 6, 12, 16, 18, react at 100–110 °C with molybdenum dichloride, $MoCl_2$, yielding light yellow organic–inorganic hybrid salts, $[C_n\text{mim}]_2[\{Mo_6\}Cl_{14}]$. Crystal structures were solved for the first two members of the series. For **1**, two modifications were secured, of which **1a** was the least thermodynamically stable, although with the highest density, due to the partly *gauche* conformation of the butyl side chain. Salts with longer alkyl chains solidified into wax-like compounds and had rather complicated thermal behaviour, resulting in thermotropic LC behaviour for $[C_n\text{mim}]_2[\{Mo_6\}Cl_{14}]$ (n = 16 and 18). All five salts showed a bright red luminescence, centred at around 730 nm, upon excitation either into the imidazolium head group (475 nm) or into cluster based levels at 360 nm. Lifetimes decreased from 0.154 to 0.132 ms and the length of the alkyl side chain of the cation was subject to enhanced vibronic quenching.

Experimental Section

General: All reaction products were insensitive to the constituents of air. Handling for further analyses was undertaken in air, unless mentioned otherwise.

Materials: 1-Methylimidazole (> 99%, Sigma Aldrich), 1-chlorobutane (99+%, Acros Organics), 1-chlorohexane (95%, Acros Organics), 1-chlorododecane (99%, Acros Organics), 1-chlorohexadecane (≥ 97%, Fluka), 1-chlorooctadecane (≥ 97%, Fluka), CH_2Cl_2 (99.99%, Fisher Scientific) and acetone (p.a., Fisher Scientific) were used as received. Acetonitrile (99.5%, J. T. Baker) and toluene (99.5%, Prolabo) were dried prior to use.

Syntheses: Syntheses were carried by using standard Schlenk and argon glovebox techniques.

$[C_n\text{mim}]Cl$: Following a common literature procedure,[8] 1-methylimidazole (1 equiv.) and the respective chloroalkane (1 equiv.) were heated in acetonitrile at reflux for 3 d. After cooling, the mixture was slowly added to cold toluene (–30 °C). The white precipitate was filtered off quickly and dried under vacuum. $[C_6\text{mim}]Cl$ was obtained as a viscous and colourless liquid.

$[C_4\text{mim}]Cl$: ^{1}H NMR [298 K, 250 MHz, $CDCl_3$ (99.8%, Deutero GmbH)]: δ = 0.9 (s, H), 1.3 (m, H), 1.8 (m, H), 4.0 (s, H), 4.2 (t, $^3J_{H,H}$ = Hz, H), 7.2 (d, $^3J_{H,H}$ = Hz, H), 7.2 (d, $^3J_{H,H}$ = Hz, H), 10.9 (s, H) ppm.

$[C_6\text{mim}]Cl$: ^{1}H NMR [300 MHz, D_2O (99.9%, Deutero GmbH)]: δ = 0.78 (t, $^3J_{H,H}$ = Hz, 3 H); 1.22 (m, 6 H); 1.80 (t, $^3J_{H,H}$ = Hz, 2 H); 3.83 (s, 3 H); 4.13 (t, $^3J_{H,H}$ = Hz, 2 H); 7.40 (d, $^3J_{H,H}$ = Hz, 2 H); 8.67 (s, 1 H) ppm.

$[C_{12}\text{mim}]Cl$: ^{1}H NMR [298 K, 250 MHz, D_2O (99.9%, Deutero GmbH)]: δ = 0.74 (t, $^3J_{H,H}$ = Hz, 3 H); 1.12 (s, 20 H); 3.83 (s, 3 H); 4.1 (t, $^3J_{H,H}$ = Hz, 2 H), 7.44 (d, $^3J_{H,H}$ = Hz, 1 H); 7.48 (d, $^3J_{H,H}$ = Hz, 1 H) ppm.

$[C_{16}\text{mim}]Cl$: ^{1}H NMR [298 K, 250 MHz, D_2O (99.9%, Deutero GmbH)]: δ = 0.74 (t, $^3J_{H,H}$ = Hz, 3 H), 1.21 (s, 28 H); 3.84 (s, 3 H); 4.16 (t, $^3J_{H,H}$ = Hz, 2 H), 7.44 (d, $^3J_{H,H}$ = Hz, 1 H), 7.48 (d, $^3J_{H,H}$ = Hz, 1 H) ppm.

$[C_{18}\text{mim}]Cl$: ^{1}H NMR [298 K, 250 MHz, D_2O (99.9%, Deutero GmbH)]: δ = 0.75 (t, $^3J_{H,H}$ = Hz, 3 H); 1.16 (s, 32 H); 3.84 (s, 3 H); 4.16 (t, $^3J_{H,H}$ = Hz, 2 H), 7.44 (d, $^3J_{H,H}$ = Hz, 1 H), 7.48 (d, $^3J_{H,H}$ = Hz, 1 H) ppm.

$MoCl_2$: The synthesis succeeded by a conproportionation reaction of $MoCl_5$ and Mo at 850 °C in a sealed silica ampoule.[16] The reaction product was checked for identity and phase purity by X-ray powder diffraction. The recorded powder pattern compared well with data from the PDF database and can be found in the Supporting Information.

$[C_n\text{mim}]_2[Mo_6Cl_{14}]$, n = 4, 6, 12, 16 or 18: An excess of $[C_n\text{mim}]Cl$ and $MoCl_2$ were reacted in a Schlenk tube under vacuum at 100–110 °C in an oil bath for 3 d. After allowing the reaction mixtures to cool to room temperature in the oil bath, compounds **1a** and **2** were obtained as orange block-shaped crystals and (due to the smaller particle size) a lighter, yellow powder, respectively. Compounds **3**, **4** and **5** formed as waxy, sticky orange solids. For further purification, the solids were washed with water and filtered. The solid residue was washed off the filter with CH_2Cl_2 or acetone. The respective solvent was then removed under reduced pressure and the remaining solids were dried for several hours at 100 °C.

$[C_4\text{mim}]_2[Mo_6Cl_{14}]$ (1): $C_{16}H_{30}Cl_{14}Mo_6N_4$ (1350.42): calcd. C 14.23, N 4.15, H 2.24; found C 14.26, N 4.16, H 2.34.

$[C_6\text{mim}]_2[Mo_6Cl_{14}]$ (2): $C_{20}H_{38}Cl_{14}Mo_6N_4$ (1406.53): calcd. C 17.08, N 3.98, H 2.72; found C 17.38, N 3.93, H 2.73.

$[C_{12}\text{mim}]_2[Mo_6Cl_{14}]$ (3): $C_{32}H_{62}Cl_{14}Mo_6N_4$ (1574.85): calcd. C 26.64, N 3.45, H 3.85; found C 26.25, N 3.84, H 4.28.

$[C_{16}\text{mim}]_2[Mo_6Cl_{14}]$ (4): $C_{40}H_{78}Cl_{14}Mo_6N_4$ (1687.07): calcd. C 28.55, N 3.33, H 4.43; found C 29.19, N 3.33, H 5.44.

$[C_{18}\text{mim}]_2[Mo_6Cl_{14}]$ (5): $C_{44}H_{86}Cl_{14}Mo_6N_4$ (1743.17): calcd. C 30.32, N 3.21, H 4.97; found C 31.86, N 3.26, H 5.83.

$[C_4\text{mim}]_2[Mo_6Cl_{14}]$: A second modification of **1b** was obtained by reacting $MoCl_2$ in a 0.5 mol-% excess of $[C_4\text{mim}]Cl$ in a sealed ampoule for 24 h at 130 °C in an oven. After cooling at 2 °C h^{-1}, orange crystals were obtained. Estimated yield: 75%. $C_{16}H_{30}Cl_{14}Mo_6N_4$ (1350.42): calcd. C 14.23, N 4.15, H 2.24; found C 16.43, N 4.75, H 2.86.

Powder X-ray Diffraction: Powder X-ray diffraction data were obtained by using an image plate Guinier diffractometer (Huber G 670, Rimsting; Mo-$K_{\alpha 1}$). Temperature-dependent SAXS experiments were carried out at the A2 Beamline of DORIS III, Hasylab, DESY, Hamburg, Germany, at a fixed wavelength of 1.5 Å. The data were collected with a MarCCD detector. The detector was calibrated with silver behenate. The sample–detector position was fixed at 635.5 mm. For measurements, the samples were placed in a copper sample holder between aluminium foil. The sample temperature was controlled by a JUMO IMAGO 500 multi-channel process and program controller. Data reduction and analysis, correction or background scattering and transmission were carried out by using a2tool (Hasylab).

Crystal Structure Determinations: A few crystals of **1a** were selected under perfluorinated polyether (viscosity 1600 cSt, ABCR GmbH, Karlsruhe) with the aid of an optical microscope. The best specimen was chosen and adhered to a glass capillary with oil. A complete intensity data set was collected by using a Bruker smart 1000 single-crystal X-ray diffractometer (Bruker, Karlsruhe) with graphite-monochromated Mo-K_α radiation (λ = 0.71073 Å) at –60 °C. Data reduction was carried out with the program package SAINT[17] and a numerical absorption correction with the program SADABS.[18]

For data collection for **1b**, single crystals were sealed in Lindemann glass capillaries of 0.2 mm o.d. and, for **2**, crystals were selected again under perfluorinated polyether. Data collection was performed on a IPDS-I single-crystal diffractometer (Stoe, Darmstadt). Data reduction was carried out with the program package X-AREA[19] and a numerical absorption correction with the program X-RED.[20]

Crystal structure solutions by direct methods using SIR 92[21] yielded heavy-atom positions. Subsequent difference Fourier analyses and least-squares refinement with SHELXL-97[22] allowed the location of the remaining atom positions. In the final step of the crystal structure refinement, hydrogen atoms of idealized –CH, $–CH_2$ and $–CH_3$ groups were added and treated with the riding atom mode; their isotropic displacement factor was chosen to be 1.2 (–CH, $–CH_2$) and 1.5 ($–CH_3$) times the preceding carbon atom. For further information see the Supporting Information.

CCDC-12345 (for **1a**), -12345 (for **1b**) and -12345 (**2**) contain supplementary crystallographic data for this paper. These data can be obtained free of charge from The Cambridge Crystallographic Data Centre via www.ccdc.cam.ac.uk/data_request/cif. For drawings of the crystal structure the program DIAMOND[23] was used.

Differential Scanning Calorimetry (DSC): Melting point and phase-transition determinations were performed on a DSC 204 F1 Phoenix instrument (Netzsch-Gerätebau GmbH, Selb). The samples were sealed under argon in aluminium crucibles. Measurements were carried out with a thermal ramp of 5 K min^{-1} for **1a**, **2**, **3** and 10 K min^{-1} for **1b**, **4** and **5**.

Thermogravimetric Analysis (TG): The thermal decomposition of $[C_n\text{mim}]_2[Mo_6Cl_{14}]$ (n = 4, 18) was investigated on a TGA-50 thermoanalyzer (Shimadzu, Scientific Instruments, USA) using alumina crucibles as sample holders. The samples were heated at 5 K min^{-1}. Nitrogen was used as the purge gas during the measurements. The thermal decomposition of $[C_n\text{mim}]_2[Mo_6Cl_{14}]$ (n = 6, 12, 16) was investigated on a NETZSCH STA 409C/CD (Netzsch-Gerätebau GmbH, Selb, D) using alumina crucibles as sample holders. The samples were heated at 5 K min^{-1}. Argon was used as the purge gas during the measurements.

UV/Vis Absorption Spectroscopy: Absorption spectra in the visible range were measured at room temperature on a Cary 5000 spectrometer (Varian, Palo Alto, USA). For measurements, small amounts of $[C_n\text{mim}]_2[Mo_6Cl_{14}]$ (n = 4, 6, 12, 16, 18) were mixed carefully with KCl (analytical grade, Riedel-de Haën) and pressed (Perkin–Elmer hydraulic press) to give thin pellets. The samples were placed on a solid sample holder 5 mm in diameter and fixed with silicone paste (Baysilone Paste, Bayer, Leverkusen).

Luminescence Spectroscopy: Absorption and emission spectra were recorded on a FluoroLog-3 (Horriba Jobin Yvon) spectrometer by using a 450-W xenon lamp as the excitation source and a photomultiplier as the detector. Samples of $[C_n\text{mim}]_2[Mo_6Cl_{14}]$ (n = 4, 6, 12, 16, 18) were prepared in silica tubes sealed with wax or Parafilm (Pechiney Plastic Packing).

Infrared Spectroscopy: Measurements were performed on an Alpha FT-IR spectrometer (Bruker, Karlsruhe) in the attenuated total reflection (ATR) mode. The ATR unit was equipped with a diamond crystal, which was coated with the neat sample.

Polarizing Optical Microscopy (POM): The samples for POM measurements were prepared under ambient conditions. Small amounts of $[C_n\text{mim}]_2[Mo_6Cl_{14}]$ (n = 16, 18) were placed between thin glass slides under a microscope equipped with crossed polarizers and a video camera (Axio Imager A1, Zeiss). For heating and cooling of the samples, a THMS 600 (Linkam Scientific Instruments, GB) heating and cooling stage was used. The measurements were carried out at a thermal ramp of 5 K min^{-1}.

Supporting Information (see footnote on the first page of this article): X-ray powder diffraction patterns, IR spectra, absorption spectra and thermoanalytical data (TG, DSC) for all compounds.

Acknowledgments

This work has been supported by the State of Nordrhein-Westfalen through the Universities of Cologne and Bochum, especially within the framework of the Collaborative Research Program 608 (Complex transition metal compounds with spin and charge degrees of freedom and disorder) and the Priority Program SPP 1191 (Ionic Liquids) supported by the Deutsche Forschungsgemeinschaft (DFG), Bonn. A. V. M. is grateful for a Dozentenstipendium awarded by the Fonds der Chemischen Industrie, Frankfurt/Main.

[1] a) H. Schäfer, H. G. Schnering, *Angew. Chem.* **1964**, *76*, 833–849; b) J. D. Corbett, *Acc. Chem. Res.* **1981**, *14*, 239–246; c) J. D. Corbett, *J. Chem. Soc., Dalton Trans.* **1996**, 575–587; d) J. D. Corbett, *Inorg. Chem.* **2000**, *39*, 5178–5191; e) J. D. Corbett, *J. Alloys Compd.* **2006**, *418*, 1–20; f) J. D. Corbett, *Inorg. Chem.* **2010**, *49*, 13–28.

[2] a) H. G. Schnering, *Z. Anorg. Allg. Chem.* **1967**, *353*, 281–310; b) H. G. Schnering, *Z. Kristallogr.* **1993**, *208*, 368–369.

[3] a) P. Pfeiffer, *Z. Anorg. Chem.* **1915**, *92*, 376–380; P. Pfeiffer, *Z. Anorg. Allg. Chem.* **1916**, *97*, 161–164; b) P. Niggli, *Z. Anorg. Allg. Chem.* **1916**, *94*, 207; c) G. Meyer, *Z. Anorg. Allg. Chem.* **2008**, *634*, 2729–2736.

[4] In a valence-bond theory picture these 24 electrons occupy 12 two-centre, two-electron (2c–2e) orbitals associated with the 12 edges of the $\{Mo_6\}$ octahedron, also called metal–metal, covalent or σ (single)bonds.

[5] H. G. Schnering, *Z. Anorg. Allg. Chem.* **1971**, *385*, 75–84.

[6] See, for example: a) P. C. Healy, D. L. Kepert, D. Taylor, A. H. White, *J. Chem. Soc., Dalton Trans.* **1973**, 646–650; b) M. Potel, C. Perrin, A. Perrin, M. Sergent, *Mater. Res. Bull.* **1986**, *21*, 1239–1245; c) M. Beran, *Dissertation*, Universität zu Köln, Cologne, Germany, **2011**.

[7] P. A. Barnard, I.-W. Sun, C. L. Hussey, *Inorg. Chem.* **1990**, *29*, 3670–3674.

[8] P. Wasserscheid, T. Welton, *Ionic Liquids in Synthesis*, Wiley-VCH, Weinheim, **2007**.

[9] a) A.-V. Mudring, A. Babai, S. Arenz, R. Giernoth, *Angew. Chem.* **2005**, *117*, 5621; *Angew. Chem. Int. Ed.* **2005**, *44*, 5485; b) B. Mallick, B. Balke, C. Felser, A.-V. Mudring, *Angew. Chem.* **2008**, *120*, 7747; *Angew. Chem. Int. Ed.* **2008**, *47*, 7635; c) B. Mallick, B. Balke, C. Felser, A.-V. Mudring, *J. Am. Chem. Soc.* **2008**, *130*, 10068; d) S.-F. Tang, A. Babai, A.-V. Mudring, *Angew. Chem.* **2008**, *120*, 7743; *Angew. Chem. Int. Ed.* **2008**, *47*, 7631; e) A. Getsis, B. Balcke, C. Felser, A.-V. Mudring, *Cryst. Growth Des.* **2009**, *9*, 4429; f) A.-V. Mudring, S. F. Tang, *Eur. J. Inorg. Chem.* **2010**, 2569; g) A.-V. Mudring, *Aust. J. Chem.* **2010**, *63*, 544.

[10] a) K. Bica, P. Gaertner, *Eur. J. Org. Chem.* **2008**, 3453–3456; b) Y. Yoshida, G. Saito, *Phys. Chem. Chem. Phys.* **2010**, *12*, 1675; c) T. Bäcker, A.-V. Mudring, *Cryst. Growth & Des.* **2011**, DOI: 10.1021/cg200326n.

[11] a) A. Babai, A.-V. Mudring, *Acta Crystallogr., Sect. E* **2005**, *61*, o1534; b) A. Getsis, A.-V. Mudring, *Acta Crystallogr., Sect. E* **2005**, *61*, o2945; c) A. Babai, A.-V. Mudring, *Z. Anorg. Allg. Chem.* **2008**, *634*, 938; d) B. Mallick, B. Balke, C. Felser, A.-V. Mudring, *J. Am. Chem. Soc.* **2008**, *130*, 10068; e) A. Getsis, A.-V. Mudring, *Cryst. Res. Technol.* **2008**, *43*, 1187.

[12] J. C. Sheldon, *Nature* **1959**, *184*, 1210.

[13] A. Getsis, A.-V. Mudring, *Z. Anorg. Allg. Chem.* **2010**, *636*, 1726.

[14] a) T. Azumi, Y. Saito, *J. Phys. Chem.* **1988**, *92*, 1715; b) H. Miki, T. Ikeyama, Y. Sasaki, T. Azumi, *J. Phys. Chem.* **1992**, *96*, 3263; c) M. Ströbele, Th. Jüstel, H. Bettentrup, H.-J. Meyer, *Z. Anorg. Allg. Chem.* **2009**, *635*, 822.

[15] a) A. W. Maverick, H. B. Gray, *J. Am. Chem. Soc.* **1981**, *103*, 1298; b) A. W. Maverick, J. S. Najdzionek, D. MacKenzie, D. G. Nocera, H. B. Gray, *J. Am. Chem. Soc.* **1983**, *105*, 1878; c) T. C. Zietlow, M. D. Hopkins, H. B. Gray, *J. Solid State Chem.* **1985**, *57*, 112.

[16] H. Schäfer, H. G. von Schnering, J. V. Tillack, F. Kuhnen, H. Wöhrle, H. Baumann, *Z. Anorg. Allg. Chem.* **1967**, *353*, 281–310.

[17] *SMART* and *SAINT*, Siemens Analytical X-ray Instruments Inc., Madison, WI, **1996**.

[18] *SADABS*, Siemens Analytical X-ray Instruments Inc., Madison, WI, **1996**.

[19] *X-Shape*, v. 1.06, Crystal Optimisation for Numerical Absorption Correction (C), Stoe & Cie GmbH, Darmstadt, **1999**; *X-Area*, v. 1.16, Stoe & Cie GmbH, Darmstadt, Germany, **2003**.

[20] *X-RED*, v. 1.22, Stoe Data Reduction Program (C), Stoe & Cie GmbH, Darmstadt, Germany, **2001**; *X-STEP32*, rev. 1.06f, STOE & Cie GmbH, Darmstadt, Germany, **2000**.

[21] SIR-92: A. Altomare, G. Cascarano, G. Giacovazzo, *J. Appl. Crystallogr.* **1993**, *26*, 343.

[22] G. M. Sheldrick, *SHELXL-97*, Programs for Crystal Structure Analysis, University of Göttingen, Germany, **1997**.

[23] K. Brandenburg, H. Putz, *DIAMOND*, Program for Crystal and Molecular Structure Visualization, Crystal Impact GbR, Bonn, Germany.

Received: April 5, 2011
Published Online: August 10, 2011

